SIAM J. APPL. MATH.
Vol. 57, No. 5, pp. 1189–1215, October 1997

AN ORGANIZING CENTER FOR WAVE BIFURCATION IN MULTIPHASE FLOW MODELS*

DAN MARCHESIN†, BRADLEY J. PLOHR‡, AND STEPHEN SCHECTER§

Abstract. We consider a one-parameter family of nonstrictly hyperbolic systems of conservation laws modeling three-phase flow in a porous medium. For a particular value of the parameter, the model has a shock wave solution that undergoes several bifurcations upon perturbation of its left and right states and the parameter. In this paper we use singularity theory and bifurcation theory of dynamical systems, including Melnikov's method, to find all nearby shock waves that are admissible according to the viscous profile criterion. We use these results to construct a unique solution of the Riemann problem for each left and right state and parameter value in a neighborhood of the unperturbed shock wave solution; together with previous numerical work, this construction completes the solution of the three-phase flow model. In the bifurcation analysis, the unperturbed shock wave acts as an organizing center for the waves appearing in Riemann solutions.

Key words. Riemann problems, shock waves, viscous profiles, Melnikov's method

AMS subject classifications. 34D30, 35L65, 35L67, 35L80, 58F14

PII. S0036139995280683

1. Introduction.

Existence, uniqueness, and well-posedness for initial-value problems for mixed elliptic-hyperbolic systems of two conservation laws are important unresolved issues. Mixed-type systems can have multiple solutions for the Cauchy problem with Riemann initial data [1, 2] even when the viscous profile admissibility criterion is employed to select physically meaningful shock waves, and despite that the systems model physical phenomena. This type of nonuniqueness is expected to occur in Stone's model for three-phase flow in porous media, a mixed-type system of common usage in petroleum engineering. Nonuniqueness contributes to doubts about the physical validity of mixed-type models and about the well-posedness of Cauchy problems with discontinuous initial data.

A different class of models, introduced by Corey [3], is also employed in petroleum engineering. These models have an umbilic point in state space, an isolated point where the characteristic speeds coincide, instead of the elliptic region typical of Stone's model. Nonuniqueness of the type mentioned above does not occur. The umbilic point is the principal organizing center for Corey models; near this point, these models behave as conservation laws with quadratic polynomial flux functions, which were analyzed in [18, 7, 9, 10, 13, 17].

*Received by the editors February 1, 1995; accepted for publication (in revised form) June 7, 1996.

http://www.siam.org/journals/siap/57-5/28068.html

†Instituto de Matemática Pura e Aplicada, Estrada Dona Castorina 110, 22460 Rio de Janeiro, RJ, Brazil (marchesi@impa.br). The research of this author was supported in part by Conselho Nacional de Desenvolvimento Científico e Tecnológico grant CNPq/NSF 910087/92-0 and Financiadora de Estudos e Projetos grant 65920311-00.

‡Departments of Mathematics and of Applied Mathematics and Statistics, State University of New York at Stony Brook, Stony Brook, NY 11794-3651 (plohr@ams.sunysb.edu). The research of this author was supported in part by National Science Foundation grant INT-9216357, US Army Research Office grant DAAL03-91-C-0027 to the Mathematical Sciences Institute of Cornell University through subcontract to the State University of New York at Stony Brook, and Applied Mathematics Subprogram of the US Department of Energy grant DE-FG02-90ER25084.

§Mathematics Department, North Carolina State University, Raleigh, NC 27695 (schecter@bifur.math.ncsu.edu). The research of this author was supported in part by National Science Foundation grants INT-9216357 and DMS-9205535.

A construction that provides unique Riemann solutions for a Corey model possessing maximal symmetry between phases was described in [8]. Despite the simplifying nature of this symmetry, which is physically unrealistic, the solutions are extremely complicated. An important tool employed to solve the Riemann problems was a computer program capable of calculating all elementary shock and rarefaction waves present in the solutions. The solutions for an $O(\epsilon)$ perturbation of this model, with ϵ being a physical parameter that breaks some of the symmetry, were found by de Souza [4] using similar techniques. However, the computer program was incapable of resolving solutions in a small region of state space because of unavoidable numerical inaccuracies. Analysis shows that this region has size $O(\epsilon^3)$ in terms of the perturbation parameter ϵ, which is restricted to be less than 0.05; the computer program could not resolve nontrivial bifurcations occurring in a range of 10^{-4}, which is comparable to its numerical accuracy.

The goal in this paper is to find solutions of Riemann problems in the small region left unresolved in [4]. For the model with $\epsilon = 0$ there is a shock wave solution with left and right states U_{-0} and U_{+0}. We prove that for each left state near U_{-0}, right state near U_{+0}, and ϵ near 0 there is a solution of the Riemann problem. This solution has a rich structure, comprising a strong shock wave near the unperturbed solution together with weak shock and rarefaction waves. The construction analyzed in this work provides a unique solution for each Riemann problem. Moreover, this solution is consistent with the global solution of [4]. One interesting feature of the solution is the occurrence of composite waves containing nonclassical (transitional) shock waves.

The analysis consists of two steps. First we consider solutions of the Rankine–Hugoniot relation near the unperturbed shock wave. The solutions constitute a four-dimensional submanifold of the space of left states, right states, shock speeds, and perturbation parameter values. Associated with each such solution is a planar dynamical system that determines its physical admissibility. Because the dynamical system for the unperturbed shock wave is degenerate in several respects, we use singularity and bifurcation theory, including Melnikov's method, to determine the regions of the manifold corresponding to admissible shock waves. The analysis is simplified by the occurrence of invariant lines in the perturbed dynamical systems. Some of the calculations needed for the analysis are carried out using the *Maple* symbolic manipulation program. In the second step, we concatenate weak rarefaction and shock waves with the perturbed shock waves to obtain the Riemann solutions. Thus the unperturbed shock wave acts as an organizing center for waves appearing in solutions of Riemann problems. We expect the method of this paper, which is similar to that employed in [16], to be useful in a wide class of systems of conservation laws.

The paper is organized as follows. In section 2 we state our main result, the existence of solutions of Riemann problems; the proof is given in subsequent sections. In section 3 we find the phase portraits for dynamical systems giving rise to shock waves that are limits of traveling waves of a parabolic system associated with the system of conservation laws. Some of the analysis is presented in section 4. The shock waves that are found to be admissible are employed in the Riemann solutions constructed in section 5. In Appendices A and B we define some special shock waves and review terminology and facts from the theory of differential equations that we use in our analysis.

2. Main result.

2.1. Problem statement. The model that we consider describes the flow of three incompressible, immiscible fluids in a porous medium. Such flow is described

by two equations, which derive from the principles of conservation of mass for each fluid together with Darcy's force law. Specifically, we adopt a Corey model [3] with quadratic permeabilities. We refer the reader to [8] for the derivation of this model. The equations have a threefold symmetry when the physical properties of the fluids are assumed to be identical; the perturbations we consider change the viscosity of one of the fluids.

More precisely, we consider the one-parameter family of conservation laws

$$U_t + F(U,\epsilon)_x = 0, \tag{2.1}$$

where $U = (u,v) \in \Delta$, $\epsilon \in (-1,\infty)$, and

$$F(U,\epsilon) := (F_1(U,\epsilon), F_2(U,\epsilon)), \tag{2.2}$$

$$F_1(U,\epsilon) := \frac{u^2}{(1+\epsilon)D(U,\epsilon)}, \tag{2.3}$$

$$F_2(U,\epsilon) := \frac{v^2}{D(U,\epsilon)}, \tag{2.4}$$

$$D(U,\epsilon) := \frac{u^2}{1+\epsilon} + v^2 + (1-u-v)^2. \tag{2.5}$$

Here u and v are the saturations of two of the phases, Δ denotes the saturation triangle

$$\Delta := \{\, (u,v) \,:\, 0 < u < 1,\ 0 < v < 1, \text{ and } 0 < u+v < 1 \,\}, \tag{2.6}$$

and $1+\epsilon$ is the ratio of the viscosities of the two phases. The system is strictly hyperbolic, i.e., the eigenvalues of the Jacobian $F_U(U,\epsilon)$ are real and distinct, for all U within the interior of Δ except the isolated umbilic point

$$U^* := \left(\frac{1+\epsilon}{3+\epsilon}, \frac{1}{3+\epsilon}\right), \tag{2.7}$$

at which the Jacobian is a multiple of the identity matrix. For $U \neq U^*$, let the eigenvalues be denoted $\lambda_k(U,\epsilon)$ for $k = 1, 2$. Within open simply connected subsets of $\Delta \backslash \{U^*\}$, we can choose smooth families of corresponding right and left eigenvectors, denoted $r_k(U,\epsilon)$ and $l_k(U,\epsilon)$, respectively.

We shall solve initial-value problems for (2.1) with data

$$U(x,0) = \begin{cases} U_L & \text{for } x < 0, \\ U_R & \text{for } x > 0 \end{cases} \tag{2.8}$$

of Riemann type. In particular, we are interested in how the solutions vary with the parameter ϵ. The Riemann solutions that we construct are composed of centered rarefaction and shock waves. All shock waves appearing in these solutions satisfy the viscous-profile admissibility criterion for the identity viscosity matrix. (This choice of viscosity matrix is made for mathematical simplicity.)

More precisely, a shock wave solution of (2.1) traveling at speed s has the form

$$U(x,t) = \begin{cases} U_- & \text{for } x < st, \\ U_+ & \text{for } x > st, \end{cases} \tag{2.9}$$

where U_-, U_+, and s are related by the Rankine–Hugoniot conditions

$$F(U_+,\epsilon) - F(U_-,\epsilon) - s(U_+ - U_-) = 0. \tag{2.10}$$

A shock wave will be called admissible if the parabolic equation

$$V_t + F(V,\epsilon)_x = V_{xx} \tag{2.11}$$

has a traveling wave solution $V(x,t) = \hat{V}(x - st)$ such that

$$\lim_{\xi \to \pm\infty} \hat{V}(\xi) = U_{\pm}. \tag{2.12}$$

Equivalently, we require that $U = \hat{V}(\xi)$ be a solution of the planar differential equation

$$\dot{U} = G(U, s, U_-, \epsilon) \tag{2.13}$$

joining the equilibrium U_- to the equilibrium U_+. Here we have used the notation

$$G(U, s, U_-, \epsilon) := F(U,\epsilon) - F(U_-,\epsilon) - s(U - U_-). \tag{2.14}$$

In (2.13) we think of s as a bifurcation parameter, so that (2.13) is a three-parameter family of bifurcation problems.

In this paper, ϵ is small and the Riemann data U_L and U_R belong to small neighborhoods of specific points U_{-0} and U_{+0}, respectively, which are defined by

$$U_{-0} := (u_{-0}, v_{-0}) = \left(\frac{\sqrt{3}}{6}, \frac{\sqrt{3}}{6}\right), \tag{2.15}$$

$$U_{+0} := (u_{+0}, v_{+0}) = \left(\frac{\sqrt{3}+1}{8}, \frac{\sqrt{3}+1}{8}\right). \tag{2.16}$$

As we shall see, the pair (U_{-0}, U_{+0}) corresponds to an admissible shock wave, for the $\epsilon = 0$ model, with propagation speed

$$s_0 := \frac{76\sqrt{3} + 116}{121}. \tag{2.17}$$

This shock wave is degenerate in several respects: at U_{-0}, $s_0 = \lambda_2$, whereas at U_{+0}, $s_0 = \lambda_2$, $l_2 F_{UU} \cdot r_2 \otimes r_2 = 0$, and $l_2(U_{+0} - U_{-0}) = 0$. In the terminology of [13, 6], the shock wave belongs to the double sonic locus $\mathcal{D}$, the right hysteresis locus $\mathcal{H}_R$, and the right secondary bifurcation locus $\mathcal{B}_R$. From the point of view of bifurcation theory, the family of differential equations $\dot{U} = G(U, s, U_{-0}, 0)$ undergoes transcritical bifurcation at U_{-0} and pitchfork bifurcation at U_{+0} as s passes s_0. In a sense, this shock wave acts as an organizing center for the bifurcations of waves appearing in Riemann solutions for the system of conservation laws (2.1).

2.2. Existence of Riemann solutions. The main result of this paper is the following.

THEOREM 2.1. *For $\epsilon > 0$ sufficiently small, there exists a neighborhood $\mathcal{N}$ of the pair (U_{-0}, U_{+0}) in $\Delta \times \Delta$ such that for all $(U_L, U_R) \in \mathcal{N}$, the Riemann problem* (2.1), (2.8) *has a solution.*

The proof of this result is given in section 5. It is based on the characterization of admissible shock waves near (U_{-0}, U_{+0}), as given in section 3 and proven in section 4.

The construction provides much detail about the Riemann solutions. There are two wave patterns: (a) a 1-family wave group on the left side of a 2-family wave group or (b) a 1-family wave group separated from a 2-family wave group by a transitional

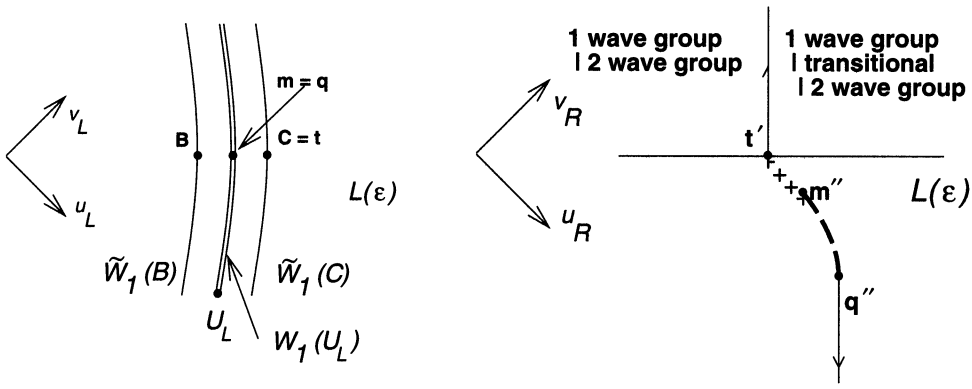

FIG. 2.1. *A simplified diagram for the case when m lies between B and C.*

wave group. In case (a), the 2-family wave group contains an admissible shock wave with left state near U_{-0} and right state near U_{+0}, whereas in case (b), it is the transitional wave group that contains such a shock wave. All other shock and rarefaction waves are weak; i.e., they are contained in a neighborhood of either U_{-0} or of U_{+0}. For each fixed U_L, there is a curve in U_R-space that separates cases (a) and (b). Each side of this curve is subdivided further according to the number and types of weak rarefaction and shock waves appearing in the transitional and 2-family wave groups. This U_R-subdivision depends on the position of U_L relative to two curves, so that there are three qualitatively distinct cases.

The subdivision into cases is explained, using diagrams, in section 5. A comparison of these diagrams with those in [4] shows that the local solution fits consistently with the global solution.

Because the solution diagrams are complicated, it is helpful to first examine a simplified diagram, Fig. 2.1. This diagram indicates the division into cases (a) and (b) for a fixed U_L that exemplifies one of the three U_L cases. (We refer the reader to Appendix A for the definitions of some special shock waves occurring in the following discussion.)

(1) There is a certain line $L(\epsilon)$ that extends through the vicinities of both U_{-0} and U_{+0}.

(2) There are precisely two points B and C on $L(\epsilon)$ near U_{-0} that are left states for admissible doubly sonic shock waves of family 2 with right states near U_{+0}.

(3) The 1-wave curve $W_1(U_L)$ through U_L intersects $L(\epsilon)$ at a unique point m. (In Fig. 2.1, we have drawn the case where m lies between B and C.) The backward 1-wave curves through B and C, $\widetilde{W}_1(B)$ and $\widetilde{W}_1(C)$, are transverse to $L(\epsilon)$, and the position of U_L relative to these curves determines the qualitative structure of the U_R-subdivision.

(4) Referring to Fig. 2.1, let q denote the rightmost of the two points B and m, and let t denote the rightmost of C and m. The point q is the left state of a unique shock wave, with right state q'' near U_{+0} but not on $L(\epsilon)$, that is right sonic in family 2. The point t is the left state of a unique shock wave, with right state $t' \in L(\epsilon)$ near U_{+0}, that undergoes secondary bifurcation in family 2 on its right side.

(5) There is a distinguished curve leading from t' to q''; each point U_+ on this curve is the right state of a shock wave with left states U_- lying along the line segment from t to q. In the situation of Fig. 2.1, there is, for each U_- between t and q, a unique

shock wave with right state U_+ near U_{+0} and speed s satisfying $\lambda_2(U_-) = s > \lambda_2(U_+)$. In particular, corresponding to $U_- = m$ is the point $U_+ = m''$. The distinguished curve comprises these points between t' and m'', whereas between m'' and q'', it comprises right states U_+ for shock waves with left state m.

(6) The curve separating case (a) from case (b) consists of the distinguished curve $t'q''$ adjoined by 2-family rarefaction curves emanating from t' and q''. If U_R lies on the left side of the separating curve, then there is a solution of the Riemann problem composed of a 1-family wave group and a 2-family wave group. If U_R lies on the right side of the separating curve, then there is a solution of the Riemann problem composed of a 1-family wave group, a 2-family wave group, and a transitional wave group between them. As U_R crosses the separating curve, the solution of the Riemann problem varies continuously (i.e., the scale-invariant solution varies continuously in L^1_{loc}).

3. Admissible shock waves.

3.1. Symmetry and degeneracy. The differential equation (2.13) has the equilibrium $U = U_-$ for each (s, U_-, ϵ). Moreover, it has certain symmetry properties, as we now describe. Define the line $L(\epsilon)$ to be

$$L(\epsilon) := \left\{ (u, v) \,:\, v = \frac{u}{1+\epsilon} \right\}. \tag{3.1}$$

Then

(1) if $U_- \in L(\epsilon)$, $L(\epsilon)$ is invariant for (2.13) for every s;

(2) if $\epsilon = 0$ and $U_- \in L(0)$, the vector field (2.13) has a reflection symmetry about $L(0)$ for every s.

To see this, it suffices to consider the auxiliary differential equation

$$\dot{U} = F(U, \epsilon) \tag{3.2}$$

and notice that $L(\epsilon)$ is an invariant line for (3.2) and that the vector field (3.2) has a reflection symmetry about $L(0)$ when $\epsilon = 0$.

We consider the bifurcation problem

$$\dot{U} = G(U, s, U_{-0}, 0), \tag{3.3}$$

for which (2.13) is an unfolding. The following statements hold, as we have verified using the *Maple* program.

(1) For the differential equation

$$\dot{U} = G(U, s_0, U_{-0}, 0), \tag{3.4}$$

(a) there are exactly two equilibria on $L(0)$, at U_{-0} and U_{+0};

(b) the equilibrium U_{-0} is a saddle-node; its center manifold can be taken to be $L(0)$, with separatrix branch joining U_{-0} to U_{+0}, and its stable manifold is perpendicular to $L(0)$;

(c) the equilibrium U_{+0} is a weak saddle point; its stable manifold is contained in $L(0)$, and its center manifold is perpendicular to $L(0)$.

(2) As s passes s_0 in the family of differential equations (3.3), the equilibrium at U_{-0} undergoes transcritical bifurcation, and the equilibrium at U_{+0} undergoes pitchfork bifurcation.

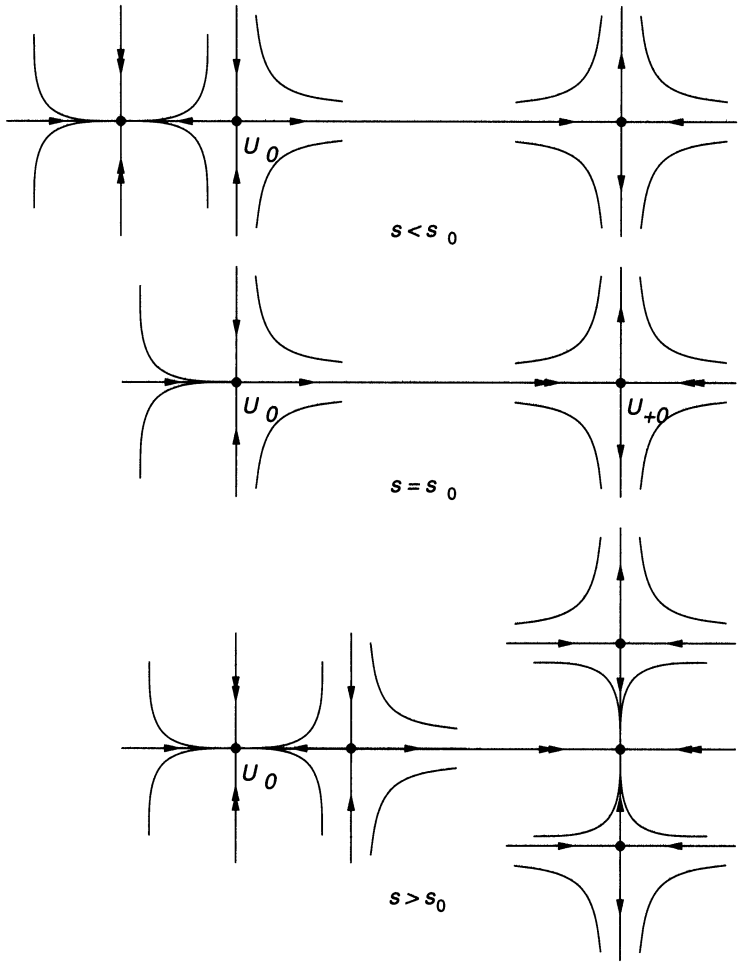

FIG. 3.1. *The phase portrait of* (3.3) *for different values of* s.

(We refer the reader to Appendix B for a summary of terminology from ordinary differential equations and bifurcation theory.) These statements are illustrated in Fig. 3.1, in which all equilibria are hyperbolic except at $s = s_0$.

The statements concerning the bifurcation problem (3.3) can be phrased in terms of geometric conditions for wave curves [19]. Property (1b) means that, for $U = U_{-0}$ and $\epsilon = 0$, $\lambda_1 < s_0 = \lambda_2$; the eigenvectors can be chosen to be $l_1 = r_1^T = (-1, 1)$ and $l_2 = r_2^T = (1, 1)$; and $l_2 F_{UU} \cdot r_2 \otimes r_2 > 0$. Similarly, property (1c) means that, for $U = U_{+0}$ and $\epsilon = 0$, $\lambda_1 < s_0 = \lambda_2$; the eigenvectors can be chosen to be $l_1 = r_1^T = (1, 1)$ and $l_2 = r_2^T = (-1, 1)$; $l_2(U_{+0} - U_{-0}) = 0$; $l_2 F_{UU} \cdot r_2 \otimes r_2 = 0$; and $l_2 F_{UUU} \cdot r_2 \otimes r_2 \otimes r_2 + 3 l_2 F_{UU} \cdot r_2 \otimes r_2' r_2 > 0$. Thus, in the terminology of [13, 6], the shock wave (U_{-0}, U_{+0}, s_0) belongs to the double sonic locus $\mathcal{D}$, the right hysteresis locus $\mathcal{H}_R$, and the right secondary bifurcation locus $\mathcal{B}_R$.

3.2. Bifurcation problem. Let $\mathcal{U}$ be a closed neighborhood in the U-plane of the line segment from U_{-0} to U_{+0}, and let $\mathcal{I} \subset \mathbb{R}$ be a closed neighborhood of s_0. The bifurcation problem (3.3) on $\mathcal{U} \times \mathcal{I}$ is actually stable to perturbations within the class of bifurcation problems that have a reflection symmetry about a

given line for each value of the bifurcation parameter. However, once symmetry-breaking perturbations, such as those that occur in the unfolding (2.13), are allowed, the bifurcation problem (3.3) must be regarded as having infinite codimension. The reason is that a saddle connection exists along the line $L(0)$ for an interval of values for s. Therefore we cannot hope to construct a universal unfolding of the bifurcation problem (3.3). (Universal unfoldings of equilibrium bifurcation problems are discussed in [5]; universal unfoldings of bifurcation problems that involve both equilibrium and separatrix connection bifurcations are discussed in [15].)

Our goal is therefore simply to analyze how the degenerate bifurcation problem (3.3) with $U \in \mathcal{U}$ and $s \in \mathcal{I}$ unfolds within the specific family (2.13). Therefore we shall study the bifurcation problem (2.13) for each fixed (U_-, ϵ) near $(U_{-0}, 0)$ and for $(U, s) \in \mathcal{U} \times \mathcal{I}$. Since transcritical bifurcations are stable to perturbation within the class of bifurcation problems that have a known "trivial equilibrium" for all values of the parameter, this bifurcation problem has a transcritical bifurcation at U_-. It also has one or more equilibrium bifurcations near U_{+0}. In addition, there may be separatrix connections from an equilibrium near U_- to one near U_{+0}.

We say that the bifurcation problem for (U_-, ϵ) is nondegenerate on $\mathcal{U} \times \mathcal{I}$ provided that

(I) the only equilibrium bifurcations that occur are the transcritical bifurcation at U_- and saddle-node bifurcations near U_{+0};

(II) the only separatrix connections that occur join saddle points, and they break in a nondegenerate manner as s varies;

(III) for each fixed s, at most one bifurcation of types mentioned in (I) and (II) occurs;

(IV) no bifurcation of type mentioned in (I) or (II) occurs on the boundary of $\mathcal{I}$, and no equilibrium or separatrix connection meets the boundary of $\mathcal{U}$.

For appropriate $\mathcal{U}$ and $\mathcal{I}$ and for (U_-, ϵ) near $(U_{-0}, 0)$, the bifurcation problem (2.13) on $\mathcal{U} \times \mathcal{I}$ is stable to perturbation if conditions (I)–(IV) hold. Condition (IV) holds for all (U_-, ϵ) sufficiently near $(U_{-0}, 0)$. Conditions (I)–(III) all fail at $(U_{-0}, 0)$.

Let us consider the possible separatrix connections in more detail. The differential equation (3.4) has equilibria at U_{-0} and U_{+0}. The center manifold $L(0)$ of U_{-0} perturbs to an invariant curve $W^c(s, U_-, \epsilon)$ of (2.13), which contains the other equilibria near U_{-0}. If $U_- \in L(\epsilon)$, then $W^c(s, U_-, \epsilon) = L(\epsilon)$ for each s. A saddle (resp., saddle-node) of (2.13) near U_{-0} has its unstable (resp., center) manifold contained in $W^c(s, U_-, \epsilon)$. On the other hand, an equilibrium Q of (2.13) near U_{+0} has a unique invariant manifold $W(Q, s, U_-, \epsilon)$ near $L(0)$: if Q is a saddle or saddle-node (resp., node), $W(Q, s, U_-, \epsilon)$ is its stable manifold (resp., strong stable manifold).

Let $\mathcal{S}_G$ denote the set of points (s, U_-, ϵ) near $(s_0, U_{-0}, 0)$ such that $W^c(s, U_-, \epsilon)$ meets $W(Q, s, U_-, \epsilon)$ for some equilibrium Q of (2.13) near U_{+0}. Clearly the set of (s, U_-, ϵ) near $(s_0, U_{-0}, 0)$ such that (2.13) has a separatrix connection in $\mathcal{U}$ is contained in $\mathcal{S}_G$. We note that in a neighborhood of $(s_0, U_{-0}, 0)$, $\{ (s, U_-, \epsilon) : U_- \in L(\epsilon) \}$ is contained in $\mathcal{S}_G$, since for such (s, U_-, ϵ), (1) $W^c(s, U_-, \epsilon) = L(\epsilon)$, (2) there is a unique equilibrium Q of (2.13) near U_{+0} in $L(\epsilon)$, and (3) $W(Q, s, U_-, \epsilon) = L(\epsilon)$. In fact we have the following proposition.

PROPOSITION 3.1. *In a neighborhood of* $(s_0, U_{-0}, 0)$, $\mathcal{S}_G = \{ (s, U_-, \epsilon) : U_- \in L(\epsilon) \}$.

The proof is deferred to section 4. Proposition 3.1 implies in particular that for (s, U_-, ϵ) near $(s_0, U_{-0}, 0)$, separatrix connections of (2.13) in $\mathcal{U}$ occur only along invariant lines, and that they do not break as s varies. Thus condition (II) can be satisfied only when separatrix connections are absent.

In a neighborhood of $(U_{-0}, 0)$ in (U_-, ϵ)-space, we define the following *transition varieties*, on which one of conditions (I)–(III) is violated:

$\mathcal{B}_G$: the closure of the set of (U_-, ϵ) for which (2.13) has a transcritical bifurcation at an equilibrium near U_{+0};

$\mathcal{H}_G$: the closure of the set of (U_-, ϵ) for which (2.13) has a hysteresis bifurcation at an equilibrium near U_{+0};

$\mathcal{D}_G$: the set of (U_-, ϵ) such that for some s, (2.13) has both a transcritical bifurcation at U_- and an equilibrium bifurcation near U_{+0}.

(The term "transition variety" and the notation $\mathcal{B}$, $\mathcal{H}$, and $\mathcal{D}$ come from [5, pp. 140 and 205].)

PROPOSITION 3.2. *In a neighborhood of* $(U_{-0}, 0)$, $\mathcal{B}_G = \{ (U_-, \epsilon) : U_- \in L(\epsilon) \}$.

The proof is deferred to section 4.

PROPOSITION 3.3. *For* (U_-, ϵ) *near* $(U_{-0}, 0)$, *the bifurcation problem* (2.13) *on* $\mathcal{U} \times \mathcal{I}$ *is degenerate if and only if* $(U_-, \epsilon) \in \mathcal{B}_G \cup \mathcal{H}_G \cup \mathcal{D}_G$.

Proof. If $(U_-, \epsilon) \notin \mathcal{B}_G \cup \mathcal{H}_G \cup \mathcal{D}_G$, (I) and (IV) are satisfied, and (III) is partially satisfied in the sense that for each s, at most one equilibrium bifurcation occurs. But Propositions 3.1 and 3.2 imply that if $(U_-, \epsilon) \notin \mathcal{B}_G$, then no separatrix connection occurs. Thus if $(U_-, \epsilon) \notin \mathcal{B}_G \cup \mathcal{H}_G \cup \mathcal{D}_G$, (II) and the rest of (III) are vacuously satisfied. □

3.3. Normal form. To analyze the bifurcation problem (2.13), we construct a pair of real-valued functions that encode the local dynamics near U_{-0} and U_{+0}. We then note that certain transformations of the function pair preserve the dynamical information. Using these manipulations, we transform the pair of functions into a simpler "normal form," which we then analyze. While our functions do not directly describe separatrix connections from equilibria near U_{-0} to equilibria near U_{+0}, Propositions 3.1 and 3.2 relate these connections to the local dynamics near U_{+0}.

We first multiply (2.13) by the factor $(1+\epsilon)^2 DD_-$, thereby clearing denominators on the right-hand side, and we absorb this factor on the left-hand side by changing the independent variable. We then define a transformation $(U, s, U_-, \epsilon) \mapsto (X, \sigma, X_-, \epsilon)$, where $X = (x, y)$ and $X_- = (x_-, y_-)$, as follows:

$$x = \quad (u - u_{+0}) + (v - v_{+0}), \tag{3.5}$$

$$y = -(u - u_{+0}) + (v - v_{+0}), \tag{3.6}$$

$$\sigma = s - s_0, \tag{3.7}$$

$$x_- = \quad (u_- - u_{-0}) + (v_- - v_{-0}), \tag{3.8}$$

$$y_- = -(u_- - u_{-0}) + (v_- - v_{-0}), \tag{3.9}$$

$$\epsilon = \epsilon. \tag{3.10}$$

We thereby obtain a family of cubic vector fields $H := (H_1, H_2)$ such that

$$\dot{X} = H(X, \sigma, X_-, \epsilon). \tag{3.11}$$

The symmetry of (2.13) when $\epsilon = 0$ and $U_- \in L(0)$ imply that the equation $\dot{X} = H(X, \sigma, X_-, 0)$ is, for each X_- on the x_--axis and each σ, symmetric about the x-axis; in particular, the x-axis is invariant. Furthermore, the statements made in section 2.1 concerning (3.3) correspond to the following facts about the equation

$$\dot{X} = H(X, \sigma, 0, 0), \tag{3.12}$$

for which (3.11) is an unfolding.

(1) For the differential equation

$$\dot{X} = H(X, 0, 0, 0), \tag{3.13}$$

(a) there are exactly two equilibria on the x-axis, for $x = x_{-0}$ and $x = 0$, where $x_{-0} := -(3 - \sqrt{3})/12$;

(b) the equilibrium at $x = x_{-0}$ is a saddle-node; its center manifold can be taken to be the x-axis, with separatrix branch joining x_{-0} to 0, and its stable manifold is the y-axis;

(c) the equilibrium at $x = 0$ is a weak saddle point; its stable manifold is contained in the x-axis, and its center manifold is tangent to the y-axis.

(2) As σ passes 0 in the family of differential equations (3.12), the equilibrium at $x = x_{-0}$ undergoes transcritical bifurcation, and the equilibrium at $x = 0$ undergoes pitchfork bifurcation.

We now analyze the bifurcations at $x = x_{-0}$ and at $x = 0$. The analysis for $x = x_{-0}$ is standard: for fixed (x_-, y_-, ϵ), (3.11) has a transcritical bifurcation at the point $X = X_-$, which corresponds to $U = U_-$, when $\sigma = \sigma^*(X_-, \epsilon) := \lambda_2(U_-, \epsilon) - s_0$. To determine orientations, we invoke property (1b) above and find that the reduced differential equation on the center manifold is equivalent to the normal form $\dot{x} = x^2 - \sigma x$, so that the bifurcation is as illustrated in Fig. 3.1 (except for a change of notation). Thus X_- is to the right of (resp., equals; resp., is to the left of) a second nearby equilibrium when σ is less than (resp., equals; resp., is greater than) $\sigma^*(X_-, \epsilon)$. Moreover, a connection near the x-axis from X_- to an equilibrium near the origin (which corresponds to $U = U_{+0}$) is possible only when X_- equals, or is to the right of, the second equilibrium. Therefore, the location of X_- relative to the nearby equilibrium is what is significant for our problem. The relative location is encoded in the function

$$k(\sigma, x_-, y_-, \epsilon) = \sigma - \sigma^*(x_-, y_-, \epsilon); \tag{3.14}$$

a connection from X_- to an equilibrium near the origin is possible only when the condition $k(\sigma, x_-, y_-, \epsilon) \leq 0$ holds.

For the bifurcation at $x = 0$, we use Liapunov–Schmidt reduction and the methods of [5]. When the center manifold is one-dimensional for each parameter value, as is the case here, Liapunov–Schmidt reduction gives exactly the same information as center manifold reduction. (This follows from Lemma 6.1 in [12].)

We begin by noting that $(H_1)_x < 0$, $(H_1)_y = 0$, and $(H_1)_\sigma < 0$ at the origin. Therefore we can solve the equation $H_1(X, \sigma, X_-, \epsilon) = 0$ for x near the origin, obtaining

$$x = \psi(y, \sigma, x_-, y_-, \epsilon), \tag{3.15}$$

where $\psi(0) = 0$ and $(\partial\psi/\partial y)(0) = 0$. Furthermore, $(\partial\psi/\partial\sigma)(0) < 0$. We then define

$$h(y, \sigma, x_-, y_-, \epsilon) := H_2(\psi(y, \sigma, x_-, y_-, \epsilon), y, \sigma, x_-, y_-, \epsilon). \tag{3.16}$$

Using the *Maple* program, we can write h and k as series in y and σ with coefficients series in the variables (X_-, ϵ). We calculate only terms of total weighted degree of at most 5, where the weights are 1 for y, 2 for σ, and 3 for x_-, y_-, and ϵ; that is, we calculate only the terms $y^i \sigma^j x_-^k y_-^l \epsilon^m$ with $i + 2j + 3k + 3l + 3m \leq 5$. The result is

(3.17)

$$\begin{aligned} h(y,\sigma,x_-,y_-,\epsilon) = {} & \left\{\left(\frac{3}{16}-\frac{1}{12}\sqrt{3}\right)y_- + \left(-\frac{1}{24}+\frac{1}{32}\sqrt{3}\right)\epsilon + \cdots\right\} \\ & + \left\{\left(-\frac{41}{48}+\frac{73}{144}\sqrt{3}\right)\epsilon + \cdots\right\} y \\ & + \left\{\left(-\frac{691}{192}+\frac{137}{64}\sqrt{3}\right)y_- - \left(\frac{131}{384}-\frac{149}{1152}\sqrt{3}\right)\epsilon + \cdots\right\}\sigma \\ & + \left\{\left(5-\frac{17}{6}\sqrt{3}\right)y_- - \left(-\frac{23}{6}+\frac{3}{2}\sqrt{3}\right)\epsilon + \cdots\right\} y^2 \\ & + \left\{-\left(-\frac{691}{48}+\frac{137}{16}\sqrt{3}\right) + \cdots\right\}\sigma y + \{0+\cdots\}\sigma^2 \\ & + \left\{\left(-14+\frac{26}{3}\sqrt{3}\right) + \cdots\right\} y^3 + \{0+\cdots\}\sigma y^2 \\ & + \left\{-\left(\frac{225803}{192}-\frac{97429}{144}\sqrt{3}\right) + \cdots\right\}\sigma^2 y + \{0+\cdots\}y^4 \\ & + \left\{\left(\frac{4661}{2}-1312\sqrt{3}\right) + \cdots\right\}\sigma y^3 \\ & + \left\{-\left(1200-592\sqrt{3}\right) + \cdots\right\} y^5 \\ & + \cdots, \end{aligned}$$

(3.18)

$$k(\sigma,x_-,y_-,\epsilon) = \sigma - \left(\frac{1212}{1331}+\frac{744}{1331}\sqrt{3}\right)x_- - \left(\frac{14}{1331}-\frac{106}{3993}\sqrt{3}\right)\epsilon + \cdots.$$

All coefficients in parentheses are positive. Since

$$h(y,\sigma,0,0,0) = -\left(-\frac{691}{48}+\frac{137}{16}\sqrt{3}\right)\sigma y + \left(-14+\frac{26}{3}\sqrt{3}\right)y^3 + \cdots, \tag{3.19}$$

there is a pitchfork bifurcation at $(y,\sigma) = (0,0)$ when $(x_-,y_-,\epsilon) = (0,0,0)$.

The mapping $(u_-,v_-,\epsilon) \mapsto (x_-,y_-,\epsilon)$ given by (3.8)–(3.10) takes $\mathcal{B}_G$, $\mathcal{H}_G$, and $\mathcal{D}_G$ to sets $\mathcal{B}_H$, $\mathcal{H}_H$, and $\mathcal{D}_H$ that have simple descriptions in terms of h and k. To simplify notation, let

$$\mu := (x_-,y_-,\epsilon). \tag{3.20}$$

Then

$$\mathcal{B}_H = \left\{\mu : \text{for some } (y,\sigma) \text{ near } (0,0),\ h = \frac{\partial h}{\partial y} = \frac{\partial h}{\partial \sigma} = 0 \text{ at } (y,\sigma,\mu)\right\}, \tag{3.21}$$

$$\mathcal{H}_H = \left\{\mu : \text{for some } (y,\sigma) \text{ near } (0,0),\ h = \frac{\partial h}{\partial y} = \frac{\partial^2 h}{\partial y^2} = 0 \text{ at } (y,\sigma,\mu)\right\}, \tag{3.22}$$

$$\mathcal{D}_H = \left\{\mu : \text{for some } (y,\sigma) \text{ near } (0,0),\ h = \frac{\partial h}{\partial y} = k = 0 \text{ at } (y,\sigma,\mu)\right\}. \tag{3.23}$$

We now apply singularity theory [5] to the functions h and k. As in [5], the function h may be transformed by an invertible transformation of the unfolding parameter μ; a μ-dependent, orientation-preserving transformation of the bifurcation parameter σ; a (σ, μ)-dependent, orientation-preserving transformation of the state variable y; and multiplication by a positive function. The function k may then be transformed using the same transformation of the unfolding parameters μ and σ, as well as multiplication by a positive function. (Recall that it is the sign of k that is significant.)

Therefore, the following equivalence relation is appropriate to our problem. Two pairs of real-valued functions $(h(y, \sigma, \mu), k(\sigma, \mu))$ and $(f(z, \lambda, \nu), g(\lambda, \nu))$, where y, z, σ, $\lambda \in \mathbb{R}$ and μ, $\nu \in \mathbb{R}^3$, are equivalent provided that there are germs of smooth mappings

$$z = Z(y, \sigma, \mu) \quad \text{with } Z(0) = 0, \ \frac{\partial Z}{\partial y}(0) > 0, \tag{3.24}$$

$$\lambda = \Lambda(\sigma, \mu) \quad \text{with } \Lambda(0) = 0, \ \frac{\partial \Lambda}{\partial \sigma}(0) > 0, \tag{3.25}$$

$$\nu = N(\mu) \quad \text{with } N(0) = 0 \text{ and } N'(0) \text{ invertible} \tag{3.26}$$

and germs of smooth real-valued functions

$$S(y, \sigma, \mu) \quad \text{with } S(0) > 0, \tag{3.27}$$

$$T(\sigma, \mu) \quad \text{with } T(0) > 0 \tag{3.28}$$

such that

$$S \cdot f(Z, \Lambda, N) = h, \tag{3.29}$$

$$T \cdot g(\Lambda, N) = k. \tag{3.30}$$

If (h, k) and (f, g) are equivalent, then the mapping $\mu \mapsto N(\mu) = \nu$ carries the sets $\mathcal{B}_H$, $\mathcal{H}_H$, and $\mathcal{D}_H$, defined as above, to sets $\mathcal{B}$, $\mathcal{H}$, and $\mathcal{D}$ defined analogously in terms of $f(z, \lambda, \nu)$ and $g(\lambda, \nu)$:

$$\mathcal{B} := \left\{ \nu : \text{for some } (z, \lambda) \text{ near } (0,0),\ f = \frac{\partial f}{\partial z} = \frac{\partial f}{\partial \lambda} = 0 \text{ at } (z, \lambda, \nu) \right\}, \tag{3.31}$$

$$\mathcal{H} := \left\{ \nu : \text{for some } (z, \lambda) \text{ near } (0,0),\ f = \frac{\partial f}{\partial z} = \frac{\partial^2 f}{\partial z^2} = 0 \text{ at } (z, \lambda, \nu) \right\}, \tag{3.32}$$

$$\mathcal{D} := \left\{ \nu : \text{for some } (z, \lambda) \text{ near } (0,0),\ f = \frac{\partial f}{\partial z} = g = 0 \text{ at } (z, \lambda, \nu) \right\}. \tag{3.33}$$

Let $\nu := (\alpha, \beta, \gamma)$ and define the pair of functions $(f(z, \lambda, \nu), g(\lambda, \nu))$ by

$$f(z, \lambda, \nu) = z^3 - \lambda z + \alpha + \beta z^2, \tag{3.34}$$

$$g(\lambda, \nu) = \lambda - \gamma. \tag{3.35}$$

PROPOSITION 3.4. *The pairs (h, k) and (f, g) are equivalent. A coordinate transformation $\Psi := (Z, \Lambda, N)$ realizing the equivalence is given, to first order, by the*

following formulas:

$$z = Z(y,\sigma,\mu) = 4\sqrt{2}\frac{a}{b}y + \frac{11\sqrt{2}}{2}\frac{a}{b^5}\left(800435 - 461916\sqrt{3}\right)y_- + \frac{\sqrt{2}}{12}\frac{a}{b^5}\left(-19561800 + 11302237\sqrt{3}\right)\epsilon + \cdots, \tag{3.36}$$

$$\lambda = \Lambda(\sigma,\mu) = \sigma - \left(\frac{76}{1331} - \frac{5}{3993}\sqrt{3}\right)\epsilon + \cdots, \tag{3.37}$$

and, with $N := (A,B,C)$,

$$\alpha = A(\mu) = 4\sqrt{2}\frac{a}{b^3}\left(9 - 4\sqrt{3}\right)y_- + 2\sqrt{2}\frac{a}{b^3}\left(-4 + 3\sqrt{3}\right)\epsilon + \cdots, \tag{3.38}$$

$$\beta = B(\mu) = \frac{\sqrt{2}}{ab^5}\left(245395893 - 141677216\sqrt{3}\right)y_- + \frac{\sqrt{2}}{2ab^5}\left(-126002996 + 72749637\sqrt{3}\right)\epsilon + \cdots, \tag{3.39}$$

$$\gamma = C(\mu) = \frac{1212 + 744\sqrt{3}}{1331}x_- - \left(\frac{62}{1331} + \frac{101}{3993}\sqrt{3}\right)\epsilon + \cdots. \tag{3.40}$$

In these equations,

$$a := \sqrt{-12 + 13\sqrt{3}}, \tag{3.41}$$

$$b := \sqrt{-691 + 411\sqrt{3}}. \tag{3.42}$$

The proof is deferred to section 4.

For the pair (f,g) of (3.34)–(3.35), it is easy to calculate that

$$\mathcal{B} = \{\nu : \alpha = 0\}, \tag{3.43}$$

$$\mathcal{H} = \left\{\nu : \alpha = \frac{\beta^3}{27}\right\}. \tag{3.44}$$

To determine $\mathcal{D}$, we note that $\mathcal{D}$ is found by simultaneously solving the equations

$$z^3 - z\lambda + \alpha + \beta z^2 = 0, \tag{3.45}$$

$$3z^2 - \lambda + 2\beta z = 0, \tag{3.46}$$

$$\lambda - \gamma = 0 \tag{3.47}$$

and projecting the solution set within (z,λ,ν)-space into ν-space. By solving the second equation for λ and substituting into the other equations, we see that $\mathcal{D}$ meets each plane $\beta =$ const. in a curve parameterized by z as follows:

$$\alpha = 2z^3 + \beta z^2, \tag{3.48}$$

$$\gamma = 3z^2 + 2\beta z. \tag{3.49}$$

This curve is regular except for a cusp at $(\alpha,\gamma) = (\beta^3/27, -\beta^2/3)$.

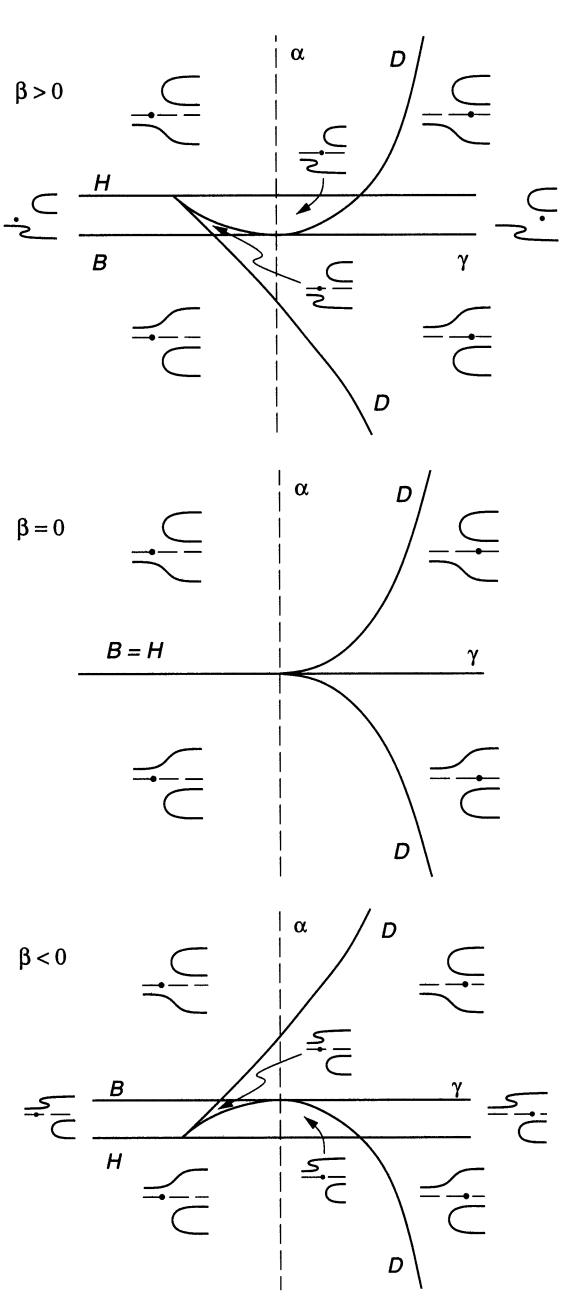

FIG. 3.2. *The transition varieties and bifurcation diagrams for the normal form pair* (f, g). *The parameter* β *is held constant in each picture.*

Each surface $\mathcal{B}$, $\mathcal{H}$, and $\mathcal{D}$ meets each plane $\beta = \text{const.}$ in a curve. The intersections of these curves are depicted in Fig. 3.2. The set $\mathcal{B} \cap \mathcal{D}$ consists of a transverse intersection at $(\alpha, \gamma) = (0, -\beta^2/4)$ and a quadratic intersection at $(\alpha, \gamma) = (0, 0)$; $\mathcal{H} \cap \mathcal{D}$ consists of the cusp in $\mathcal{D}$ and a transverse intersection at $(\alpha, \gamma) = (\beta^3/27, 5\beta^2/12)$. Notice that, in (α, β, γ)-space, $\mathcal{B} \cap \mathcal{D}$ and $\mathcal{H} \cap \mathcal{D}$ each consists of two curves tangent at the origin to the β-axis.

3.4. Projections of transition varieties. Let Φ denote the transformation from (U_-, ϵ)-space to ν-space given by

$$(U_-, \epsilon) \mapsto \mu = (x_-, y_-, \epsilon) \mapsto \nu = (\alpha, \beta, \gamma), \tag{3.50}$$

where the first arrow is given by (3.8)–(3.10) and the second arrow is given by (3.38)–(3.40). Then Φ maps a neighborhood of $(U_-, 0)$ diffeomorphically to a neighborhood of the origin, and it maps the transition varieties $\mathcal{B}_G$, $\mathcal{H}_G$, and $\mathcal{D}_G$ for the original bifurcation problem to $\mathcal{B}$, $\mathcal{H}$, and $\mathcal{D}$, respectively.

PROPOSITION 3.5. *For $|\epsilon|$ small, the sets $\mathcal{B}_G$, $\mathcal{H}_G$, and $\mathcal{D}_G$ meet a neighborhood of U_{-0} in the plane $\epsilon =$ const. in the manner shown in Fig.* 3.3.

Proof. From Proposition 3.2, $\mathcal{B}_G$ meets the plane $\epsilon =$ const. in the line $v_- = (1+\epsilon)u_-$.

Next we show that $\mathcal{H}_G$ meets the plane $\epsilon = c$ in a curve. Let S_c denote the image under Φ of this plane. It suffices to show that $\mathcal{H}$ is transverse to the plane S_0, for then $\mathcal{H}$ meets each plane S_c in a curve. To this end, notice that the transformation (3.38)–(3.40) maps a neighborhood of 0 in (x_-, y_-, ϵ)-space to a neighborhood of 0 in (α, β, γ)-space, and that its linearization at 0 takes the vectors $(1,0,0)$ and $(0,1,0)$ to the vectors

$$\left(0, 0, (1212 + 744\sqrt{3})/1331\right), \tag{3.51}$$

$$\left(4\sqrt{2}\,a\left(9 - 4\sqrt{3}\right)/b^3, \sqrt{2}\left(245395893 - 141677216\sqrt{3}\right)/(ab^5), 0\right), \tag{3.52}$$

respectively. The plane spanned by the latter vectors, namely S_0, is transverse to (β, γ)-plane, which is tangent to $\mathcal{H}$. Thus $\mathcal{H}$ is transverse to S_0.

Now we establish that $\mathcal{B}_G$ and $\mathcal{H}_G$ coincide in the plane $\epsilon = 0$ and do not meet in other planes $\epsilon =$ const. On the one hand, $\mathcal{B}_G \cap \mathcal{H}_G$ is a curve since

$$\mathcal{B}_G \cap \mathcal{H}_G = \Phi^{-1}(\mathcal{B} \cap \mathcal{H}) = \Phi^{-1}\{\,(\alpha, \beta, \gamma) \,:\, \alpha = \beta = 0\,\}. \tag{3.53}$$

On the other hand, $\mathcal{B}_G \cap \mathcal{H}_G$ is just the set of pairs (U_-, ϵ) near $(U_{-0}, 0)$ for which the bifurcation problem (2.13) has a pitchfork bifurcation near $(U, s) = (U_{+0}, s_0)$. If $\epsilon = 0$ and $U_- \in L(0)$, (2.13) is symmetric about $L(0)$ for each s, and the pitchfork bifurcation with center manifold perpendicular to $L(0)$ is stable to perturbation in the class of bifurcation problems with this symmetry. Thus the set $\{\,(U_-, 0) : U_- \in L(0),\ U_-$ near $U_{-0}\,\}$ is contained in $\mathcal{B}_G \cap \mathcal{H}_G$. Since each of these sets is a smooth curve, they are equal.

We have seen that, in (α, β, γ)-space, the sets $\mathcal{B} \cap \mathcal{D}$ and $\mathcal{H} \cap \mathcal{D}$ each consists of two curves tangent at the origin to the β-axis. Since S_0 is transverse to the β-axis, it follows that each S_c is transverse to each of these four curves. Therefore S_c, for $c \neq 0$, meets each of these curves once.

The previous remarks establish the validity of most of Fig. 3.3. We note in addition that the inverse image of the point $(0,1,0)$ under the linearization of (3.38)–(3.40) at 0 is a vector with positive ϵ-component. This is why the picture for $\epsilon > 0$ (and not $\epsilon < 0$) in Fig. 3.3 corresponds to that for $\beta > 0$ in Fig. 3.2. □

In addition to showing the sets $\mathcal{B}$, $\mathcal{H}$, and $\mathcal{D}$, Fig. 3.2 includes bifurcation diagrams for $\dot{z} = f(z, \lambda, \nu)$ with $\nu = (\alpha, \beta, \gamma)$ in various regions. The diagrams show the (λ, z)-plane, and the curves constitute the set of equilibria, i.e., z such that $f(z, \lambda, \nu) = 0$. For a λ such that there is only one equilibrium, it is a saddle point; when there are three equilibria, the outside ones (at large $|z|$) are saddle points and the middle one is

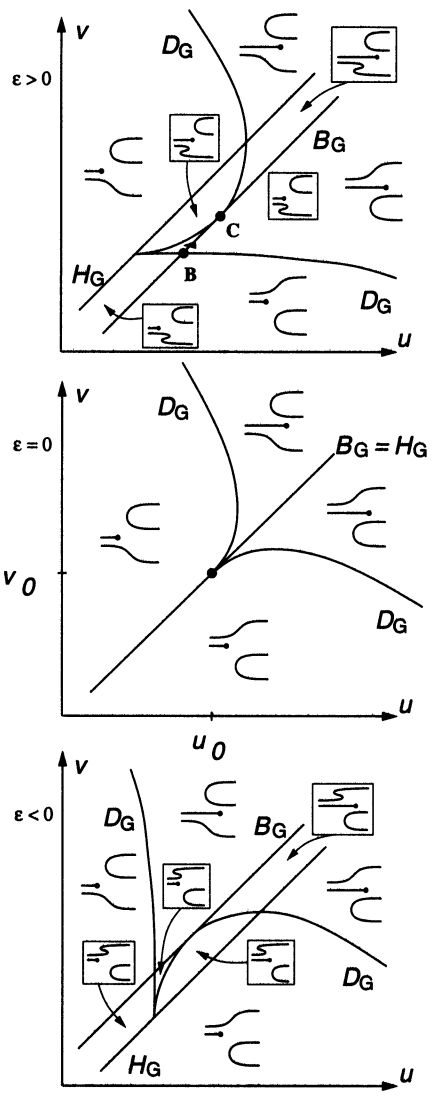

FIG. 3.3. *The transition varieties and bifurcation diagrams for the bifurcation problem* (2.13). *The parameter* ϵ *is held constant in each picture.*

an attracting node. Also shown in these diagrams is the point along the λ-axis where $g(\lambda, \nu) = 0$.

By virtue of Proposition 3.4, these diagrams correspond to equivalent ones, shown in Fig. 3.3, for the vector field $\dot{U} = G(U, s, U_-, \epsilon)$ with (U_-, ϵ) in various regions. Each diagram of Fig. 3.3 has horizontal axis being the s-interval $\mathcal{I}$ and vertical axis being the y-coordinate of U (given by (3.6)). Equations (3.36)–(3.37) define, for fixed $\mu = (U_-, \epsilon)$, the map connecting the (s, y)-diagram to the (λ, z)-diagram; notice that the derivative of this map at the origin is a diagonal matrix with positive diagonal entries. The curves correspond to equilibria near U_{+0}, and the half-line corresponds

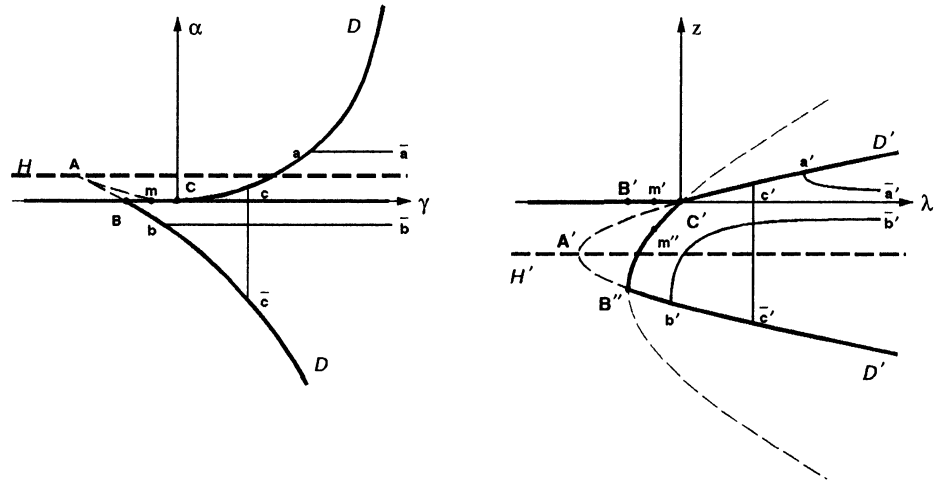

FIG. 3.4. *Curves serving as boundaries in the construction of Riemann solutions. Here* $\beta > 0$ *is fixed.*

to having $s \leq \lambda_2(U_-, \epsilon)$. For $s > \lambda_2(U_-, \epsilon)$, U_- is a node, whereas for $s < \lambda_2(U_-, \epsilon)$, U_- is a saddle point; a connection from U_- to U_+ exists only if $s \leq \lambda_2(U_-, \epsilon)$.

Each point on the half-line represents the position of the incoming separatrix from the saddle at U_-; this half-line ends in a dot, the position of the incoming separatrix from the saddle-node at U_-. The reason the half-lines are placed as drawn is that they do not meet the curves of equilibria except when $(U_-, \epsilon) \in \mathcal{B}$ (in which case the curves of equilibria contain the half-line); this is the content of Propositions 3.1 and 3.2. When $(U_-, \epsilon) \in \mathcal{B}$, the unstable manifold of U_- connects to the equilibrium on $L(\epsilon)$ near U_{+0}. When $(U_-, \epsilon) \notin \mathcal{B}$, the situation is as follows: the unstable manifold of U_- approaches a node near U_{+0} if there are three equilibria near U_{+0} and the half-line lies between two of the equilibria, but there is no connection from U_- to any U_+ if either (a) there is only one equilibrium near U_{+0} or (b) there are three equilibria near U_{+0} and the half-line lies outside all of the equilibria.

3.5. Boundary curves. The construction of Riemann solutions requires knowing several curves in the vicinity of U_{+0} that serve as boundaries separating different cases. We shall construct these boundaries using the normal form (f, g) and then transform them to the U_+-plane. Figure 3.4 shows the situation for fixed $\beta > 0$. (The case $\beta < 0$ is analogous.)

The curve $\mathcal{D}$, as projected into the (γ, α)-plane, corresponds to the curve $\mathcal{D}'$ in the (λ, z)-plane given by (3.46); the corresponding points have $\lambda = \gamma$, by (3.47). Each pair of corresponding points represents a shock wave that is doubly sonic in family 2; only for those on $\mathcal{D}B$ and $\mathcal{D}'B''$, and on $C\mathcal{D}$ and $C'\mathcal{D}'$, does the dynamical system $\dot{U} = G(U, s, U_-, \epsilon)$ have a connecting orbit joining the saddle-nodes U_- and U_+.

More generally, since f is independent of γ, the curve $\mathcal{D}'$ corresponds to turning points for f (i.e., solutions of (3.45)–(3.46)). Thus a shock wave from U_- to a state U_+ corresponding to a point on $\mathcal{D}'$ is right sonic in family 2. Such a shock wave is admissible, and of the 2-family, when U_- lies in the open region above and to the right of the curve $\mathcal{D}_G BC\mathcal{D}_G$ in Fig. 3.3.

A point in $\mathcal{H}'$ is a hysteresis point for f. Therefore, it corresponds to a state U_+ in the 2-family inflection locus, where genuine nonlinearity fails: $\lambda_2'(U_+, \epsilon) r_2(U_+, \epsilon) = 0$.

The line segment BC corresponds to several distinct curves as follows. Let $m = (\gamma, 0)$ lie on BC, and let m' lie on $B'C'$ with λ-coordinate γ. The subset of the (z, λ)-plane where $f(z, \lambda, 0, \beta, \gamma) = 0$ consists of the λ-axis and the parabola containing $B''C'$. This set represents the Hugoniot locus of the state U_- corresponding to m. The state U_+ corresponding to any point on the λ-axis to the left of C' is a saddle point, while the one corresponding to a point on $B''C'$ is a node. The only admissible shock waves for U_- correspond to points on the λ-axis to the left of m'.

The curves $B'C'$ and $B''C'$ are also obtained by another construction. Let m'' be the point on $B''C'$ with λ-coordinate γ. Then as m moves along BC, m' and m'' sweep out $B'C'$ and $B''C'$, respectively. The shock wave represented by the pair (m, m'') is of the 2-family and is left sonic; it has no viscous profile, however.

Finally, consider the curves $a\bar{a}$, $b\bar{b}$, and $c\bar{c}$. Solving (3.45) and (3.47) for fixed α yields the curves $a'\bar{a}'$, $b'\bar{b}'$, and $c'\bar{c}'$, respectively; these curves have vertical tangent in the (λ, z)-plane along $\mathcal{D}'$. A pair of corresponding points on one of these curves represents an admissible 2-family shock wave that is left sonic.

4. Proofs of Propositions 3.1, 3.2, and 3.4. We prove these propositions in reverse order.

Proof of Proposition 3.4. From (3.19), h is an unfolding of a pitchfork bifurcation. Now f is a universal unfolding of the normal form of the pitchfork; the coefficients of z^3 and λz are chosen to agree in sign with those of y^3 and σy in (3.19). According to [5], there are germs of smooth functions $Z(y, \sigma, \mu)$, $\Lambda(\sigma, \mu)$, $A(\mu)$, $B(\mu)$, and $S(y, \sigma, \mu)$, with $Z(0) = \Lambda(0) = A(0) = B(0) = 0$, $S(0) > 0$, $(\partial Z/\partial y)(0) > 0$, and $(\partial \Lambda/\partial \sigma)(0) > 0$, such that with $N = (A, B, 0)$,

$$h = S \cdot f(Z, \Lambda, N). \tag{4.1}$$

(Here we have noted that f, as defined by (3.34), is independent of γ.)

Let m denote a coordinate of μ (i.e., x_-, y_-, or ϵ). Write

$$Z(y, \sigma, 0) = a_1 y + a_2 \sigma + a_3 y^2 + \cdots, \tag{4.2}$$

$$S(y, \sigma, 0) = s_0 + s_1 y + s_2 \sigma + s_3 y^2 + \cdots, \tag{4.3}$$

$$\frac{\partial h}{\partial m}(y, \sigma, 0) = b_0^{(m)} + b_1^{(m)} y + b_2^{(m)} \sigma + b_3^{(m)} y^2 + \cdots, \tag{4.4}$$

$$\Lambda(\sigma, 0) = c_2 \sigma + \cdots. \tag{4.5}$$

Differentiate both sides of (4.1) with respect to m, set $\mu = 0$, write both sides as series in y and σ, and retain only the terms 1, y, σ, and y^2. We obtain

$$b_0^{(m)} = s_0 \frac{\partial A}{\partial m}(0), \tag{4.6}$$

$$b_1^{(m)} = -s_0 a_1 \frac{\partial \Lambda}{\partial m}(0) + s_1 \frac{\partial A}{\partial m}(0), \tag{4.7}$$

$$b_2^{(m)} = -s_0 \left(c_2 \frac{\partial Z}{\partial m}(0) + a_2 \frac{\partial \Lambda}{\partial m}(0) \right) + s_2 \frac{\partial A}{\partial m}(0), \tag{4.8}$$

$$b_3^{(m)} = s_0 \left(3a_1^2 \frac{\partial Z}{\partial m}(0) - a_3 \frac{\partial \Lambda}{\partial m}(0) + a_1^2 \frac{\partial B}{\partial m}(0) \right) - s_1 a_1 \frac{\partial \Lambda}{\partial m}(0) + s_3 \frac{\partial A}{\partial m}(0). \tag{4.9}$$

The numbers a_i, s_i, and c_2 can be determined as follows. Since $\dot{X} = H(X, \sigma, 0)$ is symmetric about the x-axis, $h(y, \sigma, 0) = -h(-y, \sigma, 0)$. Therefore

$$h(y, \sigma, 0) = y \left[y^2 g_1(y^2) - \sigma g_2(y^2, \sigma) \right], \tag{4.10}$$

where $g_1(0) = -14 + 26\sqrt{3}/3 > 0$ and $g_2(0) = -691/48 + 137\sqrt{3}/16 > 0$. We write

$$h(y,\sigma,0) = g_2(y^2,\sigma)y\left(y^2\frac{g_1(y^2)}{g_2(y^2,\sigma)} - \sigma\right), \tag{4.11}$$

which suggests choosing

$$Z(y,\sigma,0) = yg_1^{1/2}g_2^{-1/2}, \tag{4.12}$$

$$\Lambda(\sigma,0) = \sigma, \tag{4.13}$$

$$S(y,\sigma,0) = g_1^{-1/2}g_2^{3/2}. \tag{4.14}$$

It follows from Golubitsky–Schaeffer theory that any choice of functions $Z(y,\sigma,0)$, $\Lambda(\sigma,0)$, and $S(y,\sigma,0)$ that works for $\mu = 0$ can be used; we choose to use (4.12)–(4.14). Then

$$a_1 = g_1^{1/2}(0)g_2^{-1/2}(0) = \frac{4\sqrt{2}\,a}{b}, \tag{4.15}$$

$$a_2 = 0, \tag{4.16}$$

$$a_3 = \frac{1}{2}\frac{\partial^2 Z}{\partial y^2}(0) = 0, \tag{4.17}$$

$$s_0 = g_1^{-1/2}(0)g_2^{3/2}(0) = \frac{\sqrt{2}\,b^3}{384a}, \tag{4.18}$$

$$s_1 = \frac{\partial S}{\partial y}(0) = 0, \tag{4.19}$$

$$s_2 = \frac{\partial S}{\partial \sigma}(0) = \frac{\left(677409 - 389716\sqrt{3}\right)\sqrt{2}\,b}{3072a}, \tag{4.20}$$

$$s_3 = -\frac{\left(11666 - 6621\sqrt{3}\right)\sqrt{2}\,b}{32a}, \tag{4.21}$$

$$c_2 = 1. \tag{4.22}$$

The computation of the quantities s_2 and s_3 from (4.12)–(4.14) requires that we know $(\partial g_2/\partial\sigma)(0)$, $g_1''(0)$, and $(\partial^2 g_2/\partial y^2)(0)$; these are determined by the $y\sigma^2$, y^5, and $y^3\sigma$ terms of (3.17).

We can now solve the system (4.12)–(4.14) for each m. Using the results together with a_1, a_2, and (4.13), we have Z, Λ, A, and B to first order. This is how (3.36)–(3.39) are obtained.

It remains to define $T(\sigma,\mu)$ and $C(\mu)$, with $T(0) > 0$ and $C(0) = 0$, so that

$$k = T\cdot(\Lambda - C). \tag{4.23}$$

Now $k = 0$ provided that $\sigma = \sigma^*(\mu)$, where $\sigma^*(\mu)$ is given by (3.18). We define

$$\begin{aligned} C(\mu) &= \Lambda(\sigma^*(\mu),\mu) \\ &= \frac{1212 + 744\sqrt{3}}{1331}x_- + \left(-\frac{62}{1331} - \frac{101}{3993}\sqrt{3}\right)\epsilon + \cdots. \end{aligned} \tag{4.24}$$

Thus k and $\Lambda - C$ are both 0 on the set $\sigma = \sigma^*(\mu)$. Then since $[\partial(\Lambda - C)/\partial\mu](0) \neq 0$, we can find T so that (4.23) holds. One can check that the derivative of the transformation $(x_-, y_-, \epsilon) \mapsto (\alpha,\beta,\gamma)$ is invertible at the origin. □

Proof of Proposition 3.2. The bifurcation problem (3.3) has an invariant line for each s; at $s = s_0$, the equilibrium at U_{+0}, which has the invariant line as its stable manifold, undergoes a pitchfork bifurcation with center manifold transverse to the invariant line. Any perturbation of (3.3) within the class of bifurcation problems having an invariant line for each s will have a "trivial equilibrium" $U(s)$ near U_{+0} on the invariant line for all s near s_0; at some s near s_0, this equilibrium will undergo a bifurcation. On the two-dimensional parameter-dependent center manifold, both partial derivatives of the reduced vector field are zero at $(U(s), s)$. It follows that in a neighborhood of $(U_{-0}, 0)$, $\{(U_-, \epsilon) : U_- \in L(\epsilon)\} \subset \mathcal{B}_G$. Notice that this set is a two-dimensional manifold, as is $\mathcal{B}_G = \Phi^{-1}(\mathcal{B})$. Therefore, the two sets are equal. □

Proof of Proposition 3.1. We show that $\mathcal{S}_G$ is a submanifold of codimension one in (s, U_-, ϵ)-space. Since $\{(s, U_-, \epsilon) : U_- \in L(\epsilon)\}$ is contained in $\mathcal{S}_G$ and is also a submanifold of codimension one, the two sets coincide in a neighborhood of $(s_0, U_{-0}, 0)$.

To study $\mathcal{S}_G$, we first smoothly parameterize the equilibria of (2.13) near the point $(U_{+0}, s_0, U_{-0}, 0)$. From (3.17), $(\partial h/\partial \epsilon)(0) \neq 0$; then by the implicit function theorem, for $(y, \sigma, x_-, y_-, \epsilon)$ near the origin,

$$h(y, \sigma, x_-, y_-, \epsilon) = 0 \tag{4.25}$$

if and only if

$$\epsilon = \phi(y, \sigma, x_-, y_-), \tag{4.26}$$

where ϕ is smooth. The equilibria of (3.11) near the origin are thus parameterized by (y, σ, x_-, y_-) as follows:

$$\epsilon = \phi(y, \sigma, x_-, y_-), \tag{4.27}$$

$$x = \psi(y, \sigma, x_-, y_-, \phi(y, \sigma, x_-, y_-)). \tag{4.28}$$

If we then invert the transformation (3.5)–(3.10), we obtain the following parameterization by (y, σ, x_-, y_-) of the equilibria of (2.13) near $(U_{+0}, \sigma_0, U_{-0}, 0)$:

$$u = u_{+0} + \frac{1}{2}(x + y), \tag{4.29}$$

$$v = v_{+0} + \frac{1}{2}(x - y), \tag{4.30}$$

$$s = s_0 + \sigma, \tag{4.31}$$

$$u_- = u_{-0} + \frac{1}{2}(x_- + y_-), \tag{4.32}$$

$$v_- = v_{-0} + \frac{1}{2}(x_- - y_-), \tag{4.33}$$

$$\epsilon = \phi(y, \sigma, x_-, y_-), \tag{4.34}$$

where (4.28) is used to define x.

Now we apply Melnikov's method [11, 14] to find the set of points (y, σ, x_-, y_-) for which there is a separatrix connection. To simplify the notation, let

$$P := (y, \sigma, x_-, y_-); \tag{4.35}$$

also define $U(P)$ by (4.29)–(4.30) (with x given by (4.28)), $s(P)$ by (4.31), and $\mu(P)$ by (4.32)–(4.34). For the differential equation

$$\dot{U} = G(U, s(P), \mu(P)), \tag{4.36}$$

we distinguish the invariant manifolds $W^c(s(P), \mu(P))$ and $W(U(P), s(P), \mu(P))$. Let $q(t)$ denote the solution of (3.4) with $\lim_{t\to-\infty} q(t) = U_{-0}$ and $\lim_{t\to\infty} q(t) = U_{+0}$, and let N denote the line segment in the U-plane through $q(0)$ perpendicular to $L(0)$. Then $W^c(s(P), \mu(P))$ (resp., $W(U(P), s(P), \mu(P))$) meets N in a point $U_1(P)$ (resp., $U_2(P)$). We measure the separation between them by

$$d(P) = \dot{q}(0) \wedge (U_1(P) - U_2(P)); \tag{4.37}$$

here $v \wedge w$ means $\det(v, w)$. We remark that d is not smooth, but it is C^k, where k can be made arbitrarily large by restricting the neighborhood of 0 on which d is defined.

Let

$$J(t) := \exp\left(-\int_0^t \operatorname{div} G(q(s), s(0), \mu(0))\, ds\right). \tag{4.38}$$

If m denotes a coordinate of P, from the arguments of [14] it follows that

$$\begin{aligned}\frac{\partial d}{\partial m}(0) = \lim_{t\to\infty}\left[-J(t)\dot{q}(t) \wedge \frac{\partial U}{\partial m}(0)\right] \\ + \int_{-\infty}^{\infty} J(t)\dot{q}(t) \wedge \left.\frac{\partial}{\partial m}\right|_{P=0} G(q(t), s(P), \mu(P))\, dt.\end{aligned} \tag{4.39}$$

For $m = y$,

$$\left.\frac{\partial}{\partial y}\right|_{P=0} G(q(t), s(P), \mu(P)) \equiv 0, \tag{4.40}$$

since s does not depend on y, and, to first order, μ does not depend on P. On the other hand, $\lim_{t\to\infty} J(t)\dot{q}(t)$ is a positive multiple of the vector $(1, 1)$, and $(\partial U/\partial y)(0) = (1, -1)$. Therefore $(\partial d/\partial y)(0) \neq 0$.

The implicit function theorem implies that, for P near 0, $d(P) = 0$ if and only if

$$y = \tilde{\phi}(\sigma, x_-, y_-), \tag{4.41}$$

where $\tilde{\phi}$ is smooth. It follows that the transformation (3.7)–(3.10) takes $\mathcal{S}_G$ to the set of $(\sigma, x_-, y_-, \epsilon)$ such that

$$\epsilon = \phi\left(\tilde{\phi}(\sigma, x_-, y_-), \sigma, x_-, y_-\right). \tag{4.42}$$

Since this set is a C^k submanifold of codimension one in (σ, X, ϵ)-space, $\mathcal{S}_G$ is a C^k submanifold of codimension one in (s, U, ϵ)-space. □

5. Solutions of Riemann problems. In this section we describe the solutions of initial-value problems for the system of conservation laws (2.1) for initial data (2.8), thereby proving Theorem 2.1. We assume that U_L is near U_{-0}, U_R is near U_{+0}, and $\epsilon > 0$ is fixed. The solutions all contain an admissible shock wave, either of family 2 or of transitional type, with left state near U_{-0} and right state near U_{+0}; these waves have been characterized in section 3.

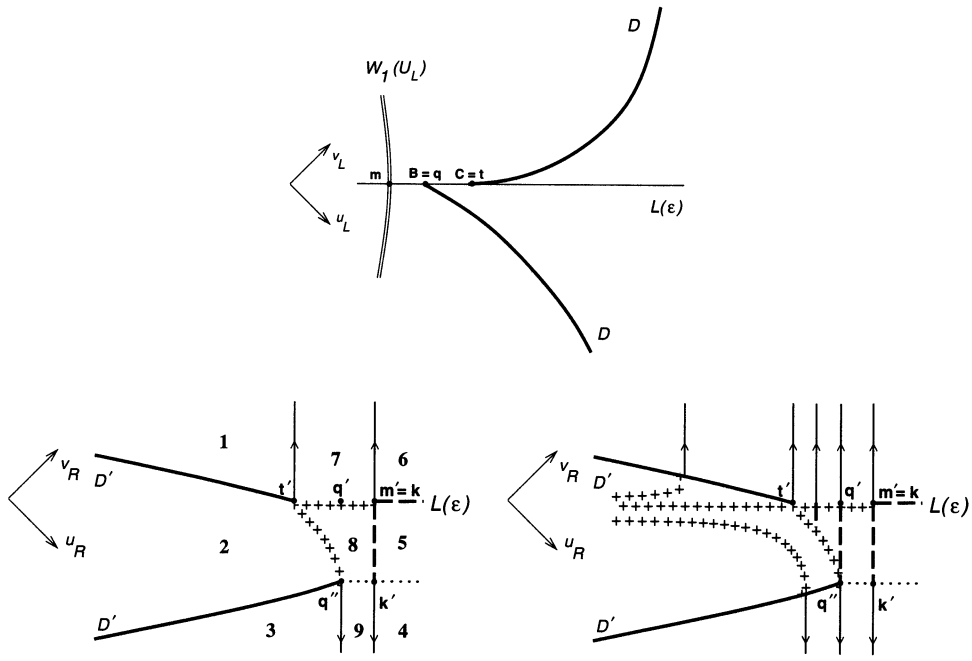

FIG. 5.1. *The case when m lies to the left of B.*

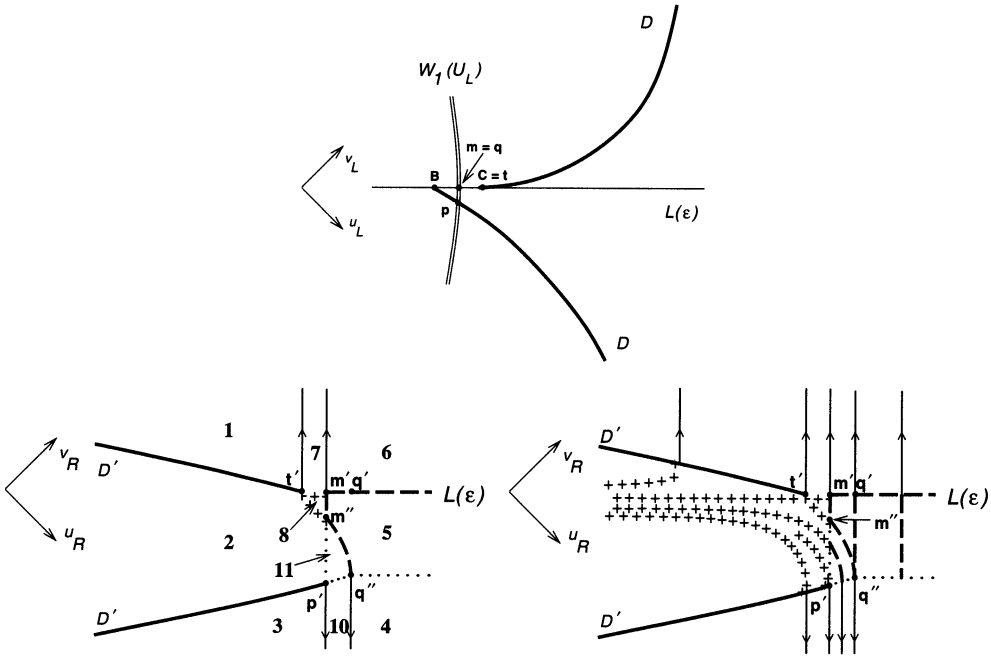

FIG. 5.2. *The case when m lies between B and C.*

5.1. Solution diagrams. The solutions are presented in Figs. 5.1–5.3. In each figure, U_L is fixed, and the corresponding wave curve of family 1, $W_1(U_L)$, is drawn in the top diagram, which shows a neighborhood of U_{-0}. The right state U_R varies

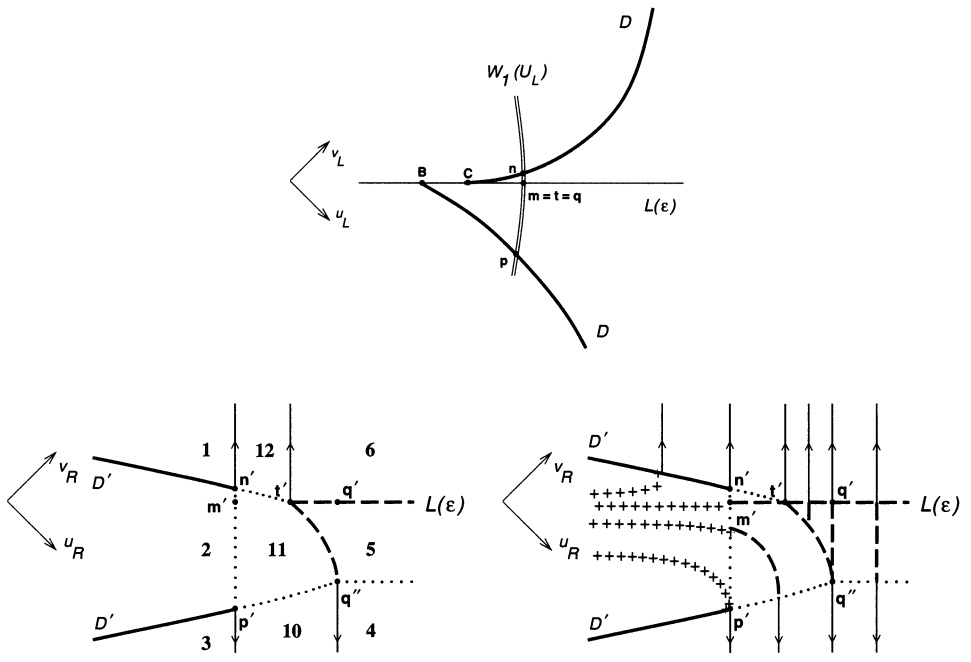

FIG. 5.3. *The case when m lies to the right of C.*

over a neighborhood of U_{+0}, which appears in the bottom two diagrams. On the bottom left we show the curves that define the boundaries of the several regions with distinct solution constructions. On the bottom right we indicate the structure of Riemann problem solutions by drawing representative wave curves of family 2 and of transitional type. Curves with arrows denote 2-rarefaction curves; dashed curves denote 2-shock curves (except for some on $L(\epsilon)$ that mark transitional shock waves); a plus denotes a composite wave, i.e., a 2-rarefaction wave followed by a 2-shock wave (or transitional shock wave, if it lies on $L(\epsilon)$) that is left sonic; and dotted curves mark certain 2-shock waves that are sonic on one side or the other. Points labeled with the same letters are joined by shock waves with the same speeds; for example, the pairs of points (m, m') and (m, m'') correspond to shock waves with the same speed.

The three figures account for the three qualitatively distinct cases, which arise as follows. When $\epsilon = 0$, the 1-family eigenvector at U_{-0} is transverse to the invariant line $L(0)$. Therefore, for sufficiently small ϵ and U_L close enough to U_{-0}, $W_1(U_L)$ is transverse to the invariant line $L(\epsilon)$ at their intersection point, m. The three cases differ in the position of m relative to the points B and C of Fig. 3.3. We remark that the solutions for U_L close to U_{-0} generalize immediately to treat states U_L that are close to any U_{L0} with the following properties: (a) $W_1(U_{L0})$ crosses $L(0)$ transversally at U_{-0}; and (b) the fastest speed of the 1-wave from U_{L0} to U_{-0} is strictly less than the 2-family characteristic speed of U_{-0}. We refer the reader to [8] and [4] for details about 1-family wave curves.

To construct the solution of the Riemann problem we use certain admissible shock waves with left states near U_{-0} and right states near U_{+0}. The implication of the bifurcation diagrams in Fig. 3.3 is that such a shock wave (U_-, U_+, s) is admissible if and only if either

(1) both U_- and U_+ belong to $L(\epsilon)$ and $s \leq \lambda_2(U_-, \epsilon)$;

(2) U_- lies in the open region above and to the right of the curve $\mathcal{D}_G B C \mathcal{D}_G$, $\lambda_2(U_+, \epsilon) \leq s \leq \lambda_2(U_-, \epsilon)$, and U_+ is a node; or

(3) U_- lies on the open curves $\mathcal{D}_G B$ or $\mathcal{D}_G C$, $s = \lambda_2(U_+, \epsilon)$, and U_+ is a saddle-node.

This shock wave is of the 2-family except in situation (1) when $s < \lambda_2(U_+, \epsilon)$ and U_+ is a saddle point, in which case it is a transitional shock wave.

5.2. Solution regions. The various boundary curves shown in Figs. 5.1–5.3 correspond to those shown in Fig. 3.4. The (γ, α)-diagram of Fig. 3.4 maps to the top diagrams in Figs. 5.1–5.3, as described in Proposition 3.5, whereas the (λ, z)-diagram maps to the bottom diagrams. The latter mapping combines the equivalence (3.36)–(3.37) of the bifurcation diagrams in the (λ, z)- and (σ, y)-planes together with the replacement of σ by $x = \psi(y, \sigma, x_-, y_-, \epsilon)$; since $(\partial\psi/\partial y)(0) = 0$ and $(\partial\psi/\partial\sigma)(0) < 0$, an (x, y)-diagram is obtained from a (λ, z)-diagram by simply reversing the orientation of the horizontal axis.

The discussion of Fig. 3.4 in section 3.5 yields the following information. Shown in the top diagrams of Figs. 5.1–5.3 are the portions $\mathcal{D}$ of the left projection of the double sonic locus $\mathcal{D}_G$ that are admissible. The bottom diagrams of each figure show the right projection $\mathcal{D}'$ of the double sonic locus. (Notice, however, that in Figs. 5.2 and 5.3 the right projection of the portion of $\mathcal{D}$ between p and B is absent, as is the portion between C and n in Fig. 5.3; this is because these portions cannot be used in the solution.)

Next, consider Fig. 5.1. Each state on the line segment mq is the left state for a unique shock wave that is left sonic in family 2; the corresponding right state, which lies on $m'q'$, is a saddle point, so that this shock wave is of transitional type. By contrast, each state on qt is the left state for three left sonic shock waves of family 2. One of them is a transitional shock wave with right state lying on $q't'$. Another shock wave has as its right state a node lying on the curve $q''t'$, and the right state of the third is a saddle point; there are no viscous profiles for these two shock waves. Notice, however, that there is an admissible (local) 2-shock wave from the state on $q't'$ to the state on $q''t'$. In the same way, in Fig. 5.2, the line segment mt corresponds to the curves $m't'$ and $m''t'$.

Also, portions of the Hugoniot locus of the point m appear Figs. 5.1–5.3. The states on $L(\epsilon)$ to the right of m' are saddle points, except for those along $m't'$ in Fig. 5.3, which are nodes. For each right state along the segment $m'q'$ in Fig. 5.2 there is a shock wave from m with the same speed and with right state on $m'q''$; these right states are joined by an admissible (local) 2-shock wave. Similarly, in Fig. 5.3, the segment $t'q'$ joins to the curve $t'q''$.

5.3. Structure of solutions. We now describe the solutions for each of regions 1–12 in Figs. 5.1–5.3. For U_R in region 1, the first wave in the solution is a 1-wave from U_L to a middle state on $W_1(U_L)$; this state lies above m in Figs. 5.1 and 5.2 and above n in Fig. 5.3. The 1-wave is followed by a 2-wave group comprising a 2-rarefaction wave to a state on $\mathcal{D}$, a doubly sonic 2-shock wave to $\mathcal{D}'$, and finally a 2-rarefaction wave to U_R. The solution in region 3 is similar, except that the middle state lies below m in Fig. 5.1 and below p in Figs. 5.2 and 5.3. For U_R in region 2, the solution is a 1-wave to a middle state on $W_1(U_L)$, followed by a 2-rarefaction wave to a state that lies to the right of the curve $\mathcal{D}BC\mathcal{D}$, followed by a 2-shock wave that is left sonic. Part of the boundary of region 2, the curves $q''t'$ in Fig. 5.1 and $m''t'$ in Fig. 5.2, is the limit of points, constructed as above, as the middle state tends to m from below. Another part, the curve $p'm''$ in Fig. 5.2 (resp., $p'n'$ in Fig. 5.3),

consists of 2-shock waves, from middle states on $W_1(U_L)$ between p and m (resp., p and n), that are left sonic. On the other side of this boundary lies region 11, which is reached by 2-shock waves from middle states on $W_1(U_L)$ between p and m (resp., p and n). The shock curves in this region end when the shock waves become right sonic in family 2; this happens on the remaining boundaries of region 11, namely $p'q''$ and, in Fig. 5.3, $t'n'$. Regions 10 and 12 are reached by following each of these right sonic shock waves with a 2-rarefaction wave.

In the remaining regions, the solutions have a three-wave structure, with a transitional wave in the middle. A transitional wave is one of two types: (1) a transitional shock wave from the first middle state m to a second middle state, which lies on the dashed portion of $L(\epsilon)$ to the right of m' in Figs. 5.1 and 5.2 and t' in Fig. 5.3; or (2) a transitional composite wave, occurring in Figs. 5.1 and 5.2, which consists of a 2-rarefaction wave from the first middle state m to a state located between m and t followed by a transitional shock wave, left sonic in family 2, to a second middle state, which lies between t' and m'. In regions 6 and 7, the transitional wave is followed by a 2-rarefaction wave originating at the second middle state, whereas in regions 5 and 8 it is followed by a 2-shock wave. Some 2-shock curves in regions 5 and 8 end when the shock speeds coincide with the speed of the transitional shock wave; this occurs along the curves $q''t'$. The other 2-shock curves in regions 5 and 8 end when the shock waves become right sonic in family 2, along the dotted boundaries of these regions. The adjoining regions 4 and 9 are reached by following these right sonic 2-shock waves with 2-rarefaction waves.

Appendix A. Definitions of special shock waves. We find it convenient to make the following definitions. A shock wave with left state U_-, right state U_+, and speed s is said to be

(1) *sonic on the left in family* i if $\lambda_i(U_-) = s$;

(2) *sonic on the right in family* j if $s = \lambda_j(U_+)$;

(3) *doubly sonic in families* i *and* j (or, when $i = j$, *of family* i) if $\lambda_i(U_-) = s = \lambda_j(U_+)$;

(4) *undergoing secondary bifurcation in family* i *on its right side* provided that $s = \lambda_i(U_+)$ and $l_i(U_+)\,[U_+ - U_-] = 0$;

(5) *undergoing hysteresis bifurcation in family* i *on its right side* provided that $s = \lambda_i(U_+)$ and $l_i(U_+)F''(U_+) \cdot r_i(U_+) \otimes r_i(U_+) = 0$.

Appendix B. Terminology from ordinary differential equations. We review some terminology and facts from ordinary differential equations. Let U_0 be an equilibrium of the planar differential equation $\dot{U} = H(U)$, and let the eigenvalues of $DH(U_0)$ be λ_1 and λ_2. The equilibrium U_0 is said to be *hyperbolic* if $\Re(\lambda_i) \neq 0$, $i = 1, 2$. Suppose that both λ_i are real; then U_0 is a *saddle point* if $\lambda_1\lambda_2 < 0$, whereas it is a *node* if $\lambda_1\lambda_2 > 0$. If exactly one $\lambda_i = 0$, then U_0 is *semihyperbolic.*

Let λ_i be an eigenvalue of a saddle or the nonzero eigenvalue of a semihyperbolic equilibrium, and let V_i be a corresponding eigenvector of $DH(U_0)$; then there is a unique invariant curve through U_0 tangent to V_i, called the *stable* (resp., *unstable*) *manifold* of U_0 if $\lambda_i < 0$ (resp., $\lambda_i > 0$). Let U_0 be a node with eigenvalues $\lambda_1 < \lambda_2 < 0$ (resp., $\lambda_1 > \lambda_2 > 0$), with corresponding eigenvectors V_1 and V_2; then there is a unique invariant curve through U_0, tangent to V_1, called the *strong stable* (resp., *strong unstable*) manifold of U_0.

Let U_0 be a semihyperbolic equilibrium and let V be an eigenvector of $DH(U_0)$ for the eigenvalue 0; then there is an invariant curve through U_0 tangent to V called the *center manifold* of U_0 (which need not be unique). Let the differential equation

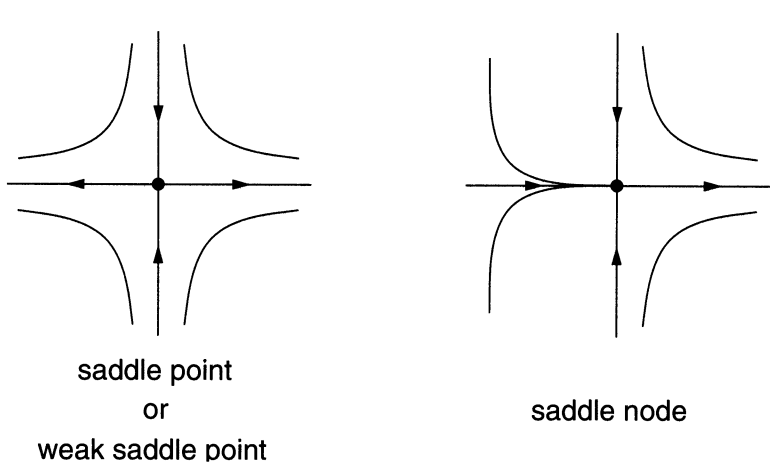

FIG. B.1. *The phase portraits of a saddle point or weak saddle point (on the left) and a saddle-node (on the right).*

on the center manifold be $\dot{x} = a_2x^2 + a_3x^3 + \cdots$, and let λ be the nonzero eigenvalue at U_0. Then U_0 is a *saddle-node* if $a_2 \neq 0$, whereas it is a *weak saddle point* if $a_2 = 0$ and $\lambda a_3 < 0$.

A solution curve that tends to U_0 as $t \to \infty$, from which some nearby solutions diverge as $t \to \infty$, is called a *separatrix*. One may replace $t \to \infty$ by $t \to -\infty$ in this definition. At a saddle point, each branch of the stable and unstable manifolds is a separatrix. At a weak saddle with a negative eigenvalue, each branch of the stable and center manifolds is a separatrix. At a saddle-node with a negative eigenvalue, each branch of the stable manifold and one branch of the center manifold is a separatrix. See Fig. B.1. Similar observations apply to weak saddle points and to saddle-nodes with a positive eigenvalue. A *separatrix connection* is a solution curve that is a separatrix as $t \to \infty$ and as $t \to -\infty$.

Let $\dot{U} = H(U, s)$ be a one-parameter family of differential equations in the plane. Suppose that for some s_0 there is a semihyperbolic equilibrium at U_0. The type of bifurcation at (U_0, s_0) is determined by the differential equation on the parameter-dependent center manifold at (U_0, s_0). In this paper we encounter the following equilibrium bifurcations (represented to lowest order in appropriate coordinates):

(B.1)	saddle-node bifurcation:	$\dot{x} = \pm s \pm x^2$;
(B.2)	transcritical bifurcation:	$\dot{x} = \pm x^2 \pm sx$;
(B.3)	hysteresis bifurcation:	$\dot{x} = \pm s \pm x^3$;
(B.4)	pitchfork bifurcation:	$\dot{x} = \pm x^3 \pm sx$.

Saddle-node bifurcations occur stably in one-parameter families. Transcritical bifurcations occur stably in families in which there is a known "trivial equilibrium" ($x = 0$ in appropriate coordinates). Pitchfork bifurcations occur stably in families with $\mathbb{Z}_2$-symmetry. If a saddle-node or transcritical bifurcation occurs at (U_0, s_0), U_0 is always a saddle-node. In this paper, whenever a hysteresis or pitchfork bifurcation occurs at (U_0, s_0), U_0 is a weak saddle point.

Acknowledgments. The authors thank Aparecido Jesuino de Souza for useful discussions about the general Riemann problem that gives rise to the bifurcation

problem treated in this paper. They also thank Sunčica Čanić for help in some of the calculations using the *Maple* program.

REFERENCES

[1] A. AZEVEDO AND D. MARCHESIN, *Multiple viscous solutions for systems of conservation laws*, Trans. Amer. Math. Soc., 347 (1995), pp. 3061–3078.

[2] A. AZEVEDO, D. MARCHESIN, B. PLOHR, AND K. ZUMBRUN, *Nonuniqueness of nonclassical solutions of Riemann problems*, Z. Angew. Math. Phys., 47 (1996), pp. 977–998.

[3] A. COREY, C. RATHJENS, J. HENDERSON, AND M. WYLLIE, *Three-phase relative permeability*, Trans. AIME, 207 (1956), pp. 349–351.

[4] A. DE SOUZA, *Stability of singular fundamental solutions under perturbations for flow in porous media*, Mat. Apl. Comput., 11 (1992), pp. 73–115.

[5] M. GOLUBITSKY AND D. SCHAEFFER, *Singularities and Groups in Bifurcation Theory*, Springer-Verlag, New York, 1984.

[6] E. ISAACSON, D. MARCHESIN, C. F. PALMEIRA, AND B. PLOHR, *A global formalism for nonlinear waves in conservation laws*, Comm. Math. Phys., 146 (1992), pp. 505–552.

[7] E. ISAACSON, D. MARCHESIN, B. PLOHR, AND J. B. TEMPLE, *The Riemann problem near a hyperbolic singularity: the classification of quadratic Riemann problems I*, SIAM J. Appl. Math., 48 (1988), pp. 1009–1032.

[8] E. ISAACSON, D. MARCHESIN, B. PLOHR, AND J. B. TEMPLE, *Multiphase flow models with singular Riemann problems*, Mat. Apl. Comput., 11 (1992), pp. 147–166.

[9] E. ISAACSON AND J. B. TEMPLE, *The Riemann problem near a hyperbolic singularity II*, SIAM J. Appl. Math., 48 (1988), pp. 1287–1301.

[10] E. ISAACSON AND J. B. TEMPLE, *The Riemann problem near a hyperbolic singularity III*, SIAM J. Appl. Math., 48 (1988), pp. 1302–1312.

[11] V. K. MELNIKOV, *On the stability of the center for time periodic perturbations*, Trans. Moscow Math. Soc., 12 (1963), pp. 1–57.

[12] D. SCHAEFFER AND M. GOLUBITSKY, *Bifurcation analysis near a double eigenvalue of a model chemical reaction*, Arch. Rational Mech. Anal., 75 (1980), pp. 315–347.

[13] D. SCHAEFFER AND M. SHEARER, *Riemann problems for nonstrictly hyperbolic* 2×2 *systems of conservation laws*, Trans. Amer. Math. Soc., 304 (1987), pp. 267–306.

[14] S. SCHECTER, *The saddle-node separatrix-loop bifurcation*, SIAM J. Math. Anal., 18 (1987), pp. 1142–1156.

[15] S. SCHECTER, *Simultaneous equilibrium and heteroclinic bifurcation of planar vector fields via the melnikov integral*, Nonlinearity, 3 (1990), pp. 79–99.

[16] S. SCHECTER AND M. SHEARER, *Undercompressive shocks for nonstrictly hyperbolic conservation laws*, J. Dynamics Differential Equations, 3 (1991), pp. 199–271.

[17] M. SPHEARER, *The Riemann problem for* 2×2 *systems of hyperbolic conservation laws with case I quadratic nonlinearities*, J. Differential Equations, 80 (1989), pp. 343–363.

[18] M. SHEARER, D. SCHAEFFER, D. MARCHESIN, AND P. PAES-LEME, *Solution of the Riemann problem for a prototype* 2×2 *system of non-strictly hyperbolic conservation laws*, Arch. Rational Mech. Anal., 97 (1987), pp. 299–320.

[19] J. SMOLLER, *Shock Waves and Reaction-Diffusion Equations*, Springer-Verlag, New York, 1983.